

Island nucleation and growth with anomalous diffusion

Jacques G. Amar^{1,*} and Mikhael Semaan^{1,2,†}

¹*Department of Physics & Astronomy, University of Toledo, Toledo, Ohio 43606, USA*

²*Department of Physics & Astronomy, California State University, Long Beach, Long Beach, California 90840, USA*

(Received 26 January 2016; revised manuscript received 15 May 2016; published 29 June 2016)

While most studies of submonolayer island nucleation and growth have been based on the assumption of ordinary monomer diffusion corresponding to diffusion exponent $\mu = 1$, in some cases either subdiffusive ($\mu < 1$) or superdiffusive ($\mu > 1$) behavior may occur. Here we present general expressions for the exponents describing the flux dependence of the island and monomer densities as a function of the critical island size i , substrate dimension d , island fractal dimension d_f , and diffusion exponent μ , where $0 \leq \mu \leq 2$. Our results are compared with kinetic Monte Carlo simulations for the case of irreversible island growth ($i = 1$) with $0 \leq \mu \leq 2$ and $d = 2$ as well as simulation results for $d = 1, 3$, and 4 , and excellent agreement is found.

DOI: [10.1103/PhysRevE.93.062805](https://doi.org/10.1103/PhysRevE.93.062805)

I. INTRODUCTION

Because of its importance in understanding and controlling thin-film growth, submonolayer island nucleation and growth has been extensively studied [1,2]. One concept of particular importance is that of a critical island size i [3] such that clusters larger than the critical island size are more likely to grow than to shrink, while clusters of size i and below are unstable. Standard rate equation (RE) theory [3] then predicts that at fixed temperature, the peak island density in the submonolayer regime scales as $N_k \sim (D/F)^{-\chi}$, where D is the monomer hopping rate, F is the (per site) deposition rate, and the exponent χ depends on the critical island size. Similarly, one may define an exponent χ_1 describing the deposition-rate dependence of the monomer density $N_1(\theta)$ at a fixed substrate coverage θ (where θ corresponds to the fraction of the substrate covered by depositing atoms or molecules) in the precoalescence regime in which the monomer density is much smaller than the island density, e.g., $N_1(\theta) \sim (D/F)^{-\chi_1}$.

For substrate dimension $d = 2$, and assuming immobile islands with fractal dimension d_f , standard RE theory [3–5] predicts that

$$\chi = 1 - \chi_1 = \frac{2i}{2i + 2 + d_f}. \quad (1)$$

One may also define the corresponding exponents χ' and χ'_1 [for which standard RE theory predicts $\chi' = 1 - \chi'_1 = i/(i + 2)$] to describe the dependence of the island and monomer densities on flux at fixed dose ϕ , where ϕ corresponds to the total coverage if all deposited particles land on the substrate. These expressions for χ , χ' , χ_1 , and χ'_1 have been confirmed in a number of theoretical and computational studies over a wide range of values of i and d_f . In addition, the expression for χ has been used in many cases, along with the scaling of the island-size distribution [6] to determine the critical island size during growth and, thus, indirectly determine the strength of atom interactions on the surface.

While these results apply to the case of ordinary monomer diffusion, such that the dependence of the mean-square monomer displacement on time t satisfies $\langle r^2(t) \rangle \sim t^\mu$ with

$\mu = 1$, there are a number of cases where anomalous diffusion may play an important role [7]. For example, recently it has been argued [8,9] that due to the existence of relatively weak molecular-substrate interactions as well as internal degrees of freedom, ballistic diffusion (corresponding to $\mu = 2$) of freshly deposited molecules may occur during the growth of pentacene and hexaphenyl on sputter-deposited mica and that this may explain the anomalously large values of the exponent χ ($\chi > 1$) observed experimentally [10,11]. A recent theoretical study [12] has also shown that underdamped Langevin diffusion on an ordered potential can give rise to superdiffusive behavior with $\mu > 1$, while similar behavior has also been observed in molecular dynamics simulations [13] of Au₁₄₀ nanoclusters on graphite. Superdiffusive behavior has also been observed experimentally [14–16] in the presence of turbulence or at a fluid interface. In contrast, it is known that in some cases of diffusion on disordered substrates, such as exciton diffusion in amorphous semiconductor films [17,18] and diffusion of “sticky” colloidal particles [19], as well as molecular diffusion in a porous medium [20], random potential [12], or biological systems [21,22], subdiffusive behavior with $\mu < 1$ may occur. Therefore, it is of interest to extend the theory of submonolayer island nucleation and growth to the more general case of anomalous monomer diffusion.

Here we derive general expressions for the exponents χ and χ_1 (as well as χ' and χ'_1) for the case of anomalous diffusion with $\mu_c \leq \mu \leq 2$ (with $\mu_c = 2/d$) which are valid for arbitrary critical island size i , substrate dimension $d \geq 1$, and island fractal dimension d_f . As a test of these predictions, we also present the results of extensive kinetic Monte Carlo simulations which were carried out for the case $i = 1$ and $d = 2$ with $1 \leq \mu \leq 2$, and excellent agreement is found. However, we also find that—due to the fact that for superdiffusion the average capture number at fixed coverage increases with decreasing deposition flux and island density—the effective value of the exponent χ only logarithmically approaches the asymptotic prediction corresponding to infinite D/F . We note that this result has important implications for the interpretation of experiments, such as those described in Refs. [10] and [11], in which it is believed that ballistic monomer diffusion may play a role. We also present results for normal diffusion in $d = 2$ which confirm the existence of logarithmic corrections in this case.

*jamar@physics.utoledo.edu

†msemaan@ucdavis.edu

Since the case of monomer subdiffusion with $\mu < 1$ is also of interest, we also present general expressions which are valid for $\mu \leq \mu_c$. Excellent agreement with the results of simulations with $i = 1$ and $d = 2$ is also found for this case. The special case of point islands ($d_f = \infty$) with $d \geq 3$ ($\mu_c = 1$) is also discussed. Our results provide a general picture of island nucleation and growth for the case of general substrate dimension, island fractal dimension, and monomer diffusion exponent μ .

II. ISLAND NUCLEATION WITH $\mu \geq \mu_c$

A. Scaling and rate-equation analysis

In order to obtain expressions for all four exponents we use a combination of scaling arguments and REs [23]. In particular, assuming that only monomers are mobile and that a critical island size i exists, in the pre-coalescence regime one may write the following set of contracted REs for the evolution of the monomer density N_1 and stable island density N (where $N = \sum_{s=2}^{\infty} N_s$, and N_s is the density of islands of size s , where s is the number of monomers in an island):

$$\frac{dN_1}{d\phi} = C_\theta - RN_1\sigma_{av}N, \quad (2a)$$

$$\frac{dN}{d\phi} = RN_1\sigma_i N_i, \quad (2b)$$

where $\phi = Ft$ and $R = D/F$, the capture numbers σ_s correspond to the propensity of an island of size s to capture a diffusing monomer, $\sigma_{av} \equiv \frac{1}{N} \sum_{s>i} \sigma_s N_s$ is the average capture number for stable islands, and $C_\theta \simeq 1 - \theta - 2R\sigma_1 N_1^2 - \sum_{s=2}^i N_s (RN_1\sigma_s - \gamma_s)$, where γ_s is the (monomer) detachment rate for islands of size $s \leq i$.

In the asymptotic limit of large D/F , one has $N_s \ll N \ll 1$ for $1 \leq s \leq i$, which implies that $C_\theta \simeq 1 - \theta$. Combining this with the steady-state assumption that at late times the rate of monomer deposition is balanced out by the rate of monomer capture implies that $\frac{dN_1}{d\phi} \simeq 0$, and one may write

$$N_1 \simeq \frac{1}{RN\sigma_{av}}. \quad (3)$$

If we substitute this expression for the monomer density N_1 into Eq. (2b) and also assume that the Walton relation [5,24] $N_i \sim N_1^i$ holds in the pre-coalescence regime, we obtain

$$\frac{dN}{d\phi} = R^{-i} \sigma_i (N\sigma_{av})^{-(i+1)}. \quad (4)$$

Since we are typically interested in the peak island density (which is determined by the onset of coalescence as a function of coverage) it is desirable to re-express this equation in terms of the effective coverage θ , which may be approximated as $\theta \simeq N(\frac{\phi}{N})^{d/d_f}$. Accordingly, we may write

$$\frac{dN}{d\theta} = \theta^{d_f/d-1} N^{1-d_f/d} \frac{dN}{d\phi}. \quad (5)$$

While the coverage dependence of σ_{av} is in general complex [2,25], here we assume that in the nucleation regime with $N \gg N_1$ and in the asymptotic limit of large D/F , for

fixed ϕ (θ) one may write

$$\sigma_{av}(\phi; N) \sim N^{-\delta/d_f}, \quad \sigma_{av}(\theta; N) \sim N^{-\delta/d}. \quad (6)$$

We note that Eq. (6) is consistent with a self-consistent RE analysis [26] that for $\mu = 1$ and $d \geq 3$ the average capture number in this regime is proportional to a power of the average cluster radius $R_{av} \sim (\frac{\phi}{N})^{1/d_f} \sim (\frac{\theta}{N})^{1/d}$.

The exponent δ may be obtained using a simple scaling argument based on the average monomer lifetime τ at fixed coverage in the aggregation regime in which $N \gg N_1$. In particular, in this regime the rate of monomer deposition is balanced by the rate of island attachment and so one may write $N_1 \simeq F\tau$. In addition, since the ratio $R_{av}/l \sim \theta^{1/d}$ (where $l = N^{-1/d}$ is the average island distance) does not depend on D/F but only depends on θ , for finite d_f and fixed coverage θ the typical distance $(D\tau)^{\mu/2}$ a monomer travels is proportional to the typical stable island distance, with a constant of proportionality that is independent of D/F , i.e., $\tau \sim D^{-1} N^{-2/\mu d}$. Combining these two expressions we obtain that, for finite d_f and fixed θ ,

$$N_1(\theta) \simeq F\tau \sim R^{-1} N(\theta)^{-2/\mu d}. \quad (7)$$

Equating this expression for N_1 with Eq. (3) and assuming $\sigma_{av}(\theta; N) \sim N^{-\delta/d}$ then leads to our main result [27]:

$$\delta = d - 2/\mu. \quad (8)$$

This implies, as expected, that for $d = 2$ and ordinary diffusion ($\mu = 1$) one has $\delta = 0$ and so the average capture number depends only logarithmically [28,29] on the average island size. It is also in agreement with the result obtained in Ref. [26] that $\delta = 1$ for ordinary diffusion in $d = 3$. The result $\delta = d - 1$ for $\mu = 2$ is also consistent with an intuitive picture of ballistic diffusion which suggests that the average capture number σ_{av} at fixed coverage θ should be proportional to the average island ‘‘cross section.’’

Equation (8) also implies the existence of a critical value $\mu_c = 2/d$ of the exponent μ such that for $\mu = \mu_c$ one has $\delta = 0$ and the standard result for χ in $d = 2$ [Eq. (1)] is obtained. More generally, for finite d_f and $\mu > \mu_c$ ($\mu < \mu_c$) one has $\delta > 0$ ($\delta < 0$) and the value of χ is higher (lower) than the critical value $\chi_c = i/(i + 1 + d_f/d)$. The dependence of δ on μ in Eq. (8) may also be expressed in terms of the random walk fractal dimension $d_w = 2/\mu$. Using this notation, one may write $\delta = d - d_w$, while the two distinct cases $\mu > \mu_c$ ($\mu < \mu_c$) correspond to $d_w < d$ ($d_w > d$), respectively.

Substituting Eq. (6) for σ_{av} , with δ given by Eq. (8) into Eq. (5) and Eq. (4), and assuming that σ_i is independent of N , and then integrating with respect to θ (ϕ), the following expressions for the exponents χ (χ') are obtained for $\mu_c \leq \mu \leq 2$ [27],

$$\chi = \frac{i\mu d}{2i + 2 + \mu d_f}, \quad \chi_1 = \frac{2 + \mu d_f}{2i + 2 + \mu d_f}, \quad (9a)$$

$$\chi' = \frac{i\mu d_f}{2i + 2 + \mu(d_f + (i + 1)\eta)}, \quad \chi'_1 = 1 - \frac{2 + \mu\eta}{\mu d_f} \chi', \quad (9b)$$

where $\eta \equiv d_f - d$. Also shown are expressions for the exponents χ_1 (χ'_1) obtained using Eq. (3). As discussed in more

detail below, for the special case of point islands ($d_f = \infty$) and $d \geq 3$, $\mu_c = 1$ rather than $2/d$.

Since Eq. (8) implies $\delta = 0$ for $d = 2$ and $\mu = 1$, these expressions are consistent with a variety of previously obtained results for the case of ordinary diffusion and substrate dimension $d = 2$. The expression for χ' in Eq. (9b) also agrees with a previous conjecture by one of us [26,30] for ordinary diffusion and substrate dimension $d \geq 2$. In addition, for the case of ballistic monomer diffusion ($\mu = 2$) we obtain $\chi = di/(i + 1 + d_f)$, which confirms and generalizes the recent prediction [9] that $\chi = 2i/(i + 3)$ for the case of ballistic diffusion with $d = d_f = 2$ to the case of general substrate dimension d and island fractal dimension d_f .

B. Simulation results

Equation (9) predicts that for point islands ($d_f = \infty$) one has $\chi' = 1 - \chi'_1 = i/(i + 2)$ for $\mu_c \leq \mu \leq 2$. We have verified that this is the case by carrying out point-island simulations for $1 \leq \mu \leq 2$ with $i = 1$ and $d = 2$. This result is also consistent with the results of previous point-island simulations [26] with $d = 3$ for the case of ordinary diffusion ($\mu = 1$) and $i = 1$.

As an additional test of these results we have carried out simulations (see Appendix A for details) for the case of irreversible growth ($i = 1$) on a two-dimensional (2D) substrate with $1 \leq \mu \leq 2$. In our simulations monomers were deposited with (per site) flux F on an initially empty substrate corresponding to an $L \times L$ lattice and were assumed to carry out nearest-neighbor hops with rate D . However, in contrast to the case of normal diffusion, in which a random hopping direction is randomly chosen at each step, in our simulations with $1 < \mu \leq 2$ the monomers executed Lévy walks [31], such that the hop direction remained constant over a persistence length l with power-law distribution $P(l) \sim l^{-(4-\mu)}$, before a new random direction was chosen [32,33].

In order to determine the asymptotic scaling behavior, simulations were carried out, with D/F ranging (in steps of $\sqrt{10}$) from 10^5 to 10^{10} . To avoid finite-size effects—which become increasingly important with increasing μ and D/F —our simulations were carried out using extremely large system sizes ($L = 45\,000$). Simulations were carried out for both ramified islands (corresponding to irreversible attachment with no cluster rearrangement and fractal dimension $d_f \simeq 1.7$ – 2.0 [34,35], depending on the coverage and dimensionality of the Lévy walk) and compact islands ($d_f = 2$), which were forced to grow in a compact spiral around each initial dimer seed.

For each value of $R = D/F$, the effective value of the exponent χ was determined using the expression $\chi(R) = -\log[N_{pk}(aR)/N_{pk}(R/a)]/\log(a^2)$ with $a = \sqrt{10}$, where $N_{pk}(u)$ corresponds to the peak island density for $D/F = u$. Similarly, the effective value of $\chi'_1(R)$ was determined for several values of ϕ in the aggregation regime corresponding to $N_1 \ll N$, using a similar expression with N_{pk} replaced by $N_1(\phi)$. However, as shown in Fig. 1—in contrast to the exponent χ'_1 , which saturates for large R —the effective value of the exponent $\chi(R)$ increases with increasing R . As also shown in Fig. 1, we have observed a similarly slow (rapid) crossover behavior for $\chi(R)$ ($\chi'_1(R)$) when numerically integrating the contracted

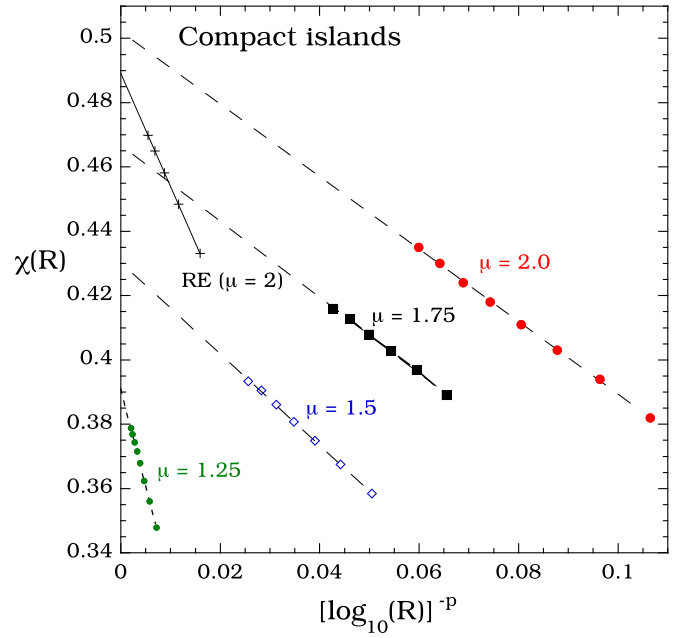


FIG. 1. Effective exponent $\chi(R)$ for $R = 10^6$ to $R = 3.16 \times 10^9$ obtained from simulations (open and filled symbols) as a function of $1/\log(R)^p$ for compact islands, where values of p correspond to best fits (dashed lines) and $\mu = 1.25$ ($p = 2.75$), $\mu = 1.5$ ($p = 1.66$), $\mu = 1.75$ ($p = 1.4$), and $\mu = 2.0$ ($p = 1.25$). Also shown are RE results for $\mu = 2$ (see text).

REs, Eq. (2), for the case $i = 1$ with $\sigma_1 = 1$, $d_f = d$, and $\delta/d = 1/2$, for which a scaling analysis [36] confirms that the corresponding asymptotic values are $\chi = 1/2$ and $\chi'_1 = 3/4$. Accordingly, in order to determine the asymptotic (large- R) value of χ , we have assumed that for finite R one may write $\chi(R) = \chi(\infty) - c/\log(R)^p$, where c and p are unknown constants. In particular, for each value of μ , we have carried out linear fits of $\chi(R)$ as a function of $\log(R)^{-p}$ for various values of p and have used the value of p which gave the best fit to the simulation data to estimate $\chi(\infty)$.

As shown in Fig. 2 there is excellent agreement between the value of χ (extrapolated) and χ'_1 obtained from our simulations of compact islands (filled circles) and ramified islands (filled triangles) [37] and the predictions of Eq. (9) with $d_f = 2$ for all values of μ between $\mu = 1$ and $\mu = 2$, except for μ close to 1. In this case our results for χ are consistent with the predicted existence [28,29] of logarithmic corrections for ordinary diffusion which lead to a somewhat larger effective value of χ . For comparison, also shown in Fig. 2 are the results obtained using a previous RE approach [32] in which the dependence of σ_{av} on N was not taken into account [dashed curves corresponding to $\chi'_1 = 2\chi = 2\mu/(1 + 2\mu)$]. In this case there is very poor agreement with our simulation results except for $\mu = 1$.

III. ISLAND NUCLEATION WITH $\mu \leq \mu_c$

A. Scaling and rate-equation analysis

While Eq. (9) holds for $\mu_c \leq \mu \leq 2$, it is also interesting to consider nucleation and growth with $\mu < \mu_c$. One example of particular interest is deposition on a 2D substrate with

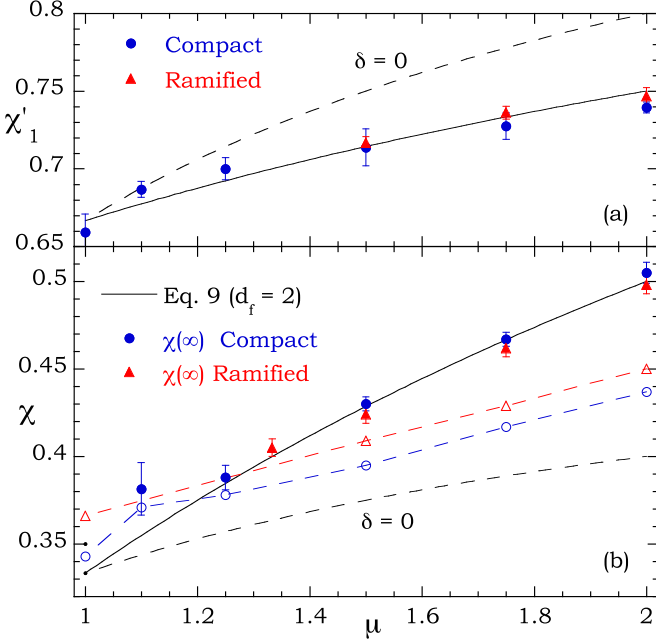


FIG. 2. Exponents χ and χ_1 obtained from simulations (symbols) for the case of superdiffusion ($1 \leq \mu \leq 2$) with $i = 1$ and $d = 2$. Solid curves correspond to Eq. (9) with $d_f = 2$. In (b) filled symbols correspond to extrapolated values, while open symbols correspond to $\chi(R)$ for the largest value of R used in our simulations. Small filled circles with $\mu = 1$ correspond to Eq. (1) with $i = 1$ and $d_f = 1.7$ (upper circle) and $d_f = 2$ (lower circle). Dashed curves labeled $\delta = 0$ correspond to RE approach [32], in which the dependence of σ_{av} on N was not taken into account.

anisotropic diffusion (or, equivalently, deposition on a 1D substrate), which corresponds to $d = 1$ and $\mu_c = 2$. Since in this case, the island radius no longer plays a direct role, it is reasonable to assume—as in previous work for the case of ordinary diffusion [38]—that at fixed coverage both σ_i and σ_{av} have the same dependence on the island density, e.g., $\sigma_i \sim \sigma_{av} \sim N^{-\delta'}$. An analysis similar to that carried out in Sec. II A then implies that $\delta' = \delta = d - 2/\mu$ with $d = 1$. We conjecture that in general for $\mu \leq \mu_c$ one has $\delta' = \delta$ rather than $\delta' = \delta/d$. Based on these assumptions we obtain [27]

$$\chi = \frac{i\mu d}{id(2 - (d-1)\mu) + \mu(d + d_f)} \quad (\mu \leq \mu_c), \quad (10a)$$

$$\chi_1' = \frac{i\mu}{i(2 - (d'-1)\mu) + 2\mu} \quad (\mu \leq \mu_c), \quad (10b)$$

with $\chi_1 = 1 - \chi(1 - \delta) = (d + d_f)\chi/(id)$ and $\chi_1' = 1 - \chi'(1 - \delta) = 2\chi'/i$. Here $d' = d$ and $\mu_c = 2/d$ for finite d_f or $d_f = \infty$ with $d \leq 2$. However, as discussed below, for the special case of point islands ($d_f = \infty$) and $d \geq 3$, $d' = 2$ and $\mu_c = 1$.

For $d = 1$ this confirms a previous result [32] for $i = d_f = 1$ and generalizes it to the case of arbitrary critical island size i and d_f . Equation (10) also implies that for $\mu \leq \mu_c$, χ_1' is independent of island fractal dimension. For $d = d_f = 2$ and $i = 1$ one has $\chi_1' = 2\chi = 2\mu/(2 + \mu)$ for $\mu \leq 1$. In contrast, assuming that for $\mu \leq \mu_c$ one has $\delta' = \delta/d$ implies that $\chi_1' = 2\chi = 2\mu/(1 + 2\mu)$ for $d = d_f = 2$ and $i = 1$.

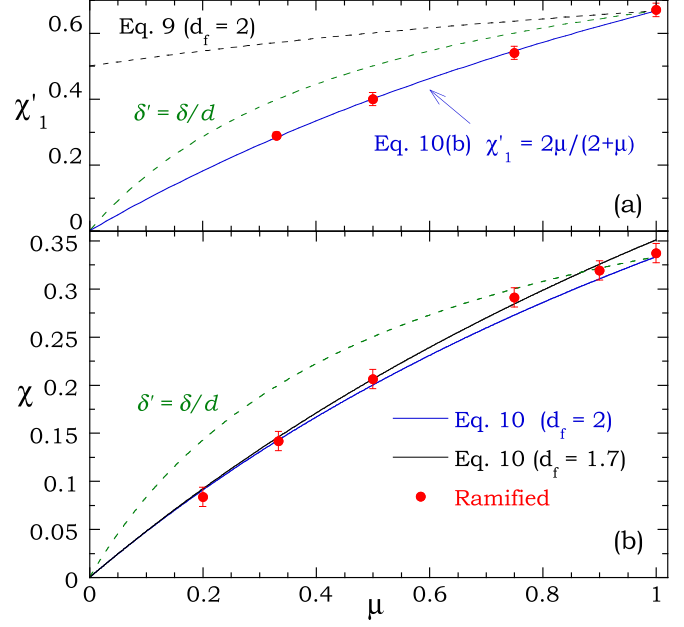


FIG. 3. Exponents χ and χ_1 as a function of μ for the case of subdiffusion ($0 \leq \mu \leq 1$) with $i = 1$ and $d = 2$. Symbols correspond to simulation results, while solid curves correspond to Eq. (10).

B. Simulation results

As a test of Eq. (10) we have carried out simulations (see Appendix B for details) of island nucleation with monomer subdiffusion ($0 \leq \mu < 1$) at $i = 1$ and $d = 2$ ($\mu_c = 1$). In our simulations, monomers were assumed to execute a continuous-time random walk [7] to nearest-neighbor sites with a power-law distribution of waiting times $P(\tau') \sim (D_0\tau')^{-1-\mu}$ and attach irreversibly to occupied nearest-neighbor sites, leading to ramified islands whose fractal dimension increases from $d_f \simeq 1.7$ as in diffusion-limited aggregation [34] to $d_f \simeq 2.0$ with increasing coverage. In order to determine the asymptotic values of χ and χ_1' very large values of D_0/F were used. We note that, in contrast to our simulation results for $\mu > 1$, in this case both χ and χ_1' saturate with increasing D_0/F . This behavior is consistent with results we have obtained for $\mu = 1/2$ with $i = 1$ by numerically integrating the contracted REs, Eq. (2), with $\delta' = -2$.

As shown in Fig. 3, there is very good agreement between the predictions of Eq. (10) for $\chi(\mu)$ and $\chi_1'(\mu)$ and our simulations [39]. In contrast, assuming that $\delta' = \delta/d$ with $d_f = 2$ (see Fig. 3) leads to poor agreement with our simulation results. Similarly, while Eq. (9) also implies $\chi = \mu/(2 + \mu)$ for $d = d_f = 2$ with $i = 1$, the corresponding prediction for χ_1' is in very poor agreement.

As a further test of Eq. (10) we have also carried out preliminary simulations with $i = 1$ and $\mu \leq 1$ for point islands in $d = 1$ and 2 , as well as for ramified islands in $d = 3$ for $\mu \leq 2/3$ [40] and have found excellent agreement in each case. However, for the special case of point islands ($d_f = \infty$) and $d \geq 2$, a monomer must visit N^{-1} rather than $N^{-2/d}$ sites before attaching to an island, which implies $\mu_c = 1$ rather than $2/d$. Since the number of sites visited in time τ for superdiffusion is equal to $D\tau$, this implies $\tau \sim N^{-1}$, $\delta = 0$, and $\chi' = 1 - \chi_1' = i/(i + 2)$ for $d_f = \infty$ and $\mu \geq \mu_c$.

Similarly, since for subdiffusion the number of sites visited in time τ is proportional to the mean-square displacement τ^μ , we obtain $\tau \sim N^{-1/\mu}$, which is equivalent to Eq. (7) with $d = 2$. This indicates that for the special case of point islands ($d_f = \infty$) in $d \geq 2$, one has $\mu_c = 1$ and $\delta' = 2 - 2/\mu$ ($\delta = 0$) for $\mu \leq \mu_c$ ($\mu \geq \mu_c$). Accordingly, we conclude that in this case the exponents χ' and χ'_1 are given by Eq. (10) (with $d' = 2$ rather than $d' = d$) for $\mu \leq 1$, while for $\mu \geq 1$, Eq. (9) holds. Simulations which we have carried out with $i = 1$, $d_f = \infty$, and $d = 3$ and 4 indicate that this is correct.

IV. DISCUSSION

We have derived expressions for the exponents describing the dependence of the monomer and island densities on deposition rate in submonolayer island growth as a function of critical island size i , substrate dimension d , and island fractal dimension d_f for the case of generalized diffusion with $0 \leq \mu \leq 2$. For the case of finite d_f , our results indicate the existence of a critical value of μ ($\mu_c = 2/d$) such that for $\mu = \mu_c$, the average capture number at fixed coverage does not depend on island density, and as a result, χ is given by the “standard” value $\chi_c = i/(i + 1 + d_f/d)$. In addition, for $\mu > \mu_c$ we obtain $\sigma_{av}(\theta; N) \sim N^{-\delta/d}$ with $\delta = d - 2/\mu > 0$, which implies that $\chi > \chi_c$. These results also imply the existence of strong crossover effects for $\mu > \mu_c$ such that the effective value of the exponent χ only logarithmically approaches the asymptotic prediction with increasing D/F . As already noted, these strong crossover effects may have important consequences for the interpretation of experiments in which anomalous monomer diffusion plays a role. For the special case of point islands ($d_f = \infty$) with $d \geq 2$, we find $\mu_c = 1$ with $\delta = 0$ for $\mu \geq 1$, which implies that $\chi' = i/(i + 2)$ for all $\mu \geq 1$.

In contrast, for $\mu < \mu_c$ our results are consistent with the assumption that $\sigma_i \sim \sigma_{av} \sim N^{-\delta'}$, where $\delta' = \delta$ rather than δ/d as expected. For finite d_f or $d_f = \infty$ with $d \leq 2$, one has $\delta' = d - 2/\mu$ and $\mu_c = 2/d$, while for $d_f = \infty$ and $d \geq 3$ we obtain $\delta' = 2 - 2/\mu$ and $\mu_c = 1$. In addition, since $\delta' < 0$ for $\mu < \mu_c$ one has $\chi(\mu) < \chi_c$ and crossover effects are significantly reduced. While we do not have an explanation for the extra factor of d in the value of δ' we conjecture that it may be related to the divergence of the mean hopping time for a continuous-time random walk with $\mu < 1$. In the future, it may be of interest to carry out simulations using correlated random walks [41] for comparison in order to gain a better understanding of the scaling behavior in this case.

It is also interesting to compare the results presented here with those obtained in previous work [32] for the case of superdiffusion ($1 \leq \mu \leq 2$) with $i = 1$. In Ref. [32], the dependence of σ_{av} and/or σ_1 on N was not taken into account, and as a result, and as shown in Fig. 2, the corresponding RE predictions for $d = 2$ with $1 < \mu \leq 2$ are incorrect. In addition, due to the small system sizes used ($L = 300$ – 1000) as well as the existence of significant crossover effects, there were significant finite-size effects in the simulations. In contrast, for the case $d = 1$ we find $\mu_c = 2$, and as a result the errors in Ref. [32] created by neglecting the N dependence of σ_1 and σ_{av} cancel out for $i = 1$. Accordingly, the predictions of Ref. [32]

for $i = d = d_f = 1$ with $1 \leq \mu \leq 2$ are in agreement with our more general results shown in Eq. (10).

Finally, we note that while these results significantly extend our understanding of island nucleation and growth, they also suggest a number of possible areas for future work. For example, while we expect, based on the arguments presented in Ref. [2], that the Walton relation holds for $\mu \neq 1$, it would be of interest to carry out simulations with $i > 1$ to check this, as well as to determine if the large crossover and finite-size effects for $i = 1$ and $\mu > \mu_c$ extend to higher critical island sizes. The dependence of the capture-number and island-size distributions on μ is also of interest and will be reported elsewhere [42]. For the case of subdiffusion due to disorder, the effects of quenched randomness in $d = 1$ are also of interest, since this may alter the scaling behavior. In addition, for the case $i = 1$, it may be possible to go beyond the asymptotic scaling results presented here by carrying out a self-consistent RE analysis (similar to that carried out for ordinary diffusion in $d = 1$ – 4 [26,29,43–45]) by solving the corresponding fractional diffusion equations for the monomer density surrounding an island. Work is currently ongoing to address these issues.

ACKNOWLEDGMENTS

This research was supported by NSF Grant No. DMR-1410840 as well as a grant of computer time from the Ohio Supercomputer Center. M.S. was supported by the Research Experience for Undergraduates (REU) program at The University of Toledo, Award No. PHY-1262810.

APPENDIX A: SUPERDIFFUSION SIMULATIONS

In our simulations for $1 < \mu \leq 2$, the persistence length l (in units of the lattice constant) was calculated using the expression $l = \xi^{-1/\beta}$, where ξ is a uniform random number between 0 and 1, and $\beta = 3 - \mu$ (see Ref. [32]). For the case $\mu = 1$ the persistence length was set to 1 (corresponding to infinite β) as in an ordinary random walk. For the case $i = 1$ and $d = 2$, our simulations of ramified, compact, and point islands were carried out using an $L \times L$ triangular lattice with periodic boundary conditions and very large system size ($L = 45\,000$) to avoid finite-size effects. As a result, in the worst possible case, corresponding to compact islands with $\mu = 2$ and $D/F = 10^{10}$, the system size L was more than 300 times the typical island distance at the peak island density. Depending on D/F , averages were taken over from 1 to 15 runs. To minimize geometric effects, in all of our point-island simulations, monomers were irreversibly “absorbed” upon landing on an already occupied (monomer or island) site whose size was then incremented by 1. As a check for the case of ramified islands with $\mu = 2$, additional simulations were carried out using a square lattice, and the results were in agreement with those obtained using a triangular lattice.

APPENDIX B: SUBDIFFUSION SIMULATIONS

In our simulations for $0 < \mu \leq 1$, the waiting time τ' was calculated using the expression $\tau' = D_0^{-1} \xi^{-1/\mu}$, where ξ is a

uniform random number between 0 and 1 and $\mu' = \mu$. In this case $\mu' < 1$ ($\mu' > 1$) corresponds to subdiffusion (ordinary diffusion), while $\mu' = 1$ corresponds to the critical value, and so logarithmic corrections are expected. All subdiffusion simulations were carried out using d -dimensional hypercubic lattices. Simulations for $i = 1$ and $d = 2$ were carried out

with D_0/F ranging from 10^{10} to a maximum value equal to 10^{16} – 10^{20} depending on the value of μ . Since finite-size effects are much weaker in this case, simulations in this case were carried out using much smaller system sizes ($L = 2048$ – 4096), while averages were typically taken over 10 runs.

-
- [1] J. W. Evans, P. A. Thiel, and M. C. Bartelt, *Surface Sci. Rep.* **61**, 1 (2006).
- [2] M. Einax, W. Dieterich, and P. Maass, *Rev. Mod. Phys.* **85**, 921 (2013).
- [3] J. A. Venables, G. D. Spiller, and M. Hanbücken, *Rep. Prog. Phys.* **47**, 399 (1984).
- [4] J. Villain, A. Pimpinelli, L.-H. Tang, and D. E. Wolf, *J. Phys. I (France)* **2**, 2107 (1992).
- [5] M. Schroeder and D. E. Wolf, *Phys. Rev. Lett.* **74**, 2062 (1995).
- [6] J. G. Amar and F. Family, *Phys. Rev. Lett.* **74**, 2066 (1995).
- [7] M. F. Shlesinger, J. Klafter, and G. Zumofen, *Am. J. Phys.* **67**, 1253 (1999).
- [8] A. Winkler and L. Tumbek, *J. Phys. Chem. Lett.* **4**, 4080 (2013).
- [9] J. R. Morales-Cifuentes, T. L. Einstein, and A. Pimpinelli, *Phys. Rev. Lett.* **113**, 246101 (2014).
- [10] L. Tumbek and A. Winkler, *Surface Sci.* **606**, L55 (2012).
- [11] A. Pimpinelli, L. Tumbek, and A. Winkler, *J. Phys. Chem. Lett.* **5**, 995 (2014).
- [12] J. M. Sancho, A. M. Lacasta, K. Lindenberg, I. M. Sokolov, and A. H. Romero, *Phys. Rev. Lett.* **92**, 250601 (2004).
- [13] W. D. Luedtke and U. Landman, *Phys. Rev. Lett.* **82**, 3835 (1999).
- [14] R. Ramshankar, D. Berlin, and J. P. Gollub, *Phys. Fluids A* **2**, 1955 (1990).
- [15] T. H. Solomon, E. R. Weeks, and H. L. Swinney, *Phys. Rev. Lett.* **71**, 3975 (1993).
- [16] H. Zheng, S. A. Claridge, A. M. Minor, A. P. Alivisatos, and U. Dahmen, *Nano Lett.* **9**, 2460 (2009).
- [17] G. Pfister and H. Scher, *Adv. Phys.* **27**, 747 (1978).
- [18] H. Scher, M. F. Shlesinger, and J. T. Bendler, *Phys. Today* **44**(1), 26 (1992).
- [19] Q. Xu, L. Feng, R. Sha, N. C. Seeman, and P. M. Chaikin, *Phys. Rev. Lett.* **106**, 228102 (2011).
- [20] G. Drazer and D. H. Zanette, *Phys. Rev. E* **60**, 5858 (1999).
- [21] I. Goychuk and V. O. Kharchenko, *Phys. Rev. Lett.* **113**, 100601 (2014).
- [22] E. Yamamoto, T. Akimoto, M. Yasui, and K. Yasuoka, *Scientific Reports* **4**, 4720 (2014).
- [23] While this approach is not sufficient to determine the detailed evolution of the island and monomer densities, it is sufficient to determine the asymptotic dependence on the deposition flux.
- [24] D. Walton, *J. Chem. Phys.* **37**, 2182 (1962).
- [25] M. Körner, M. Einax, and P. Maass, *Phys. Rev. B* **86**, 085403 (2012).
- [26] J. Royston and J. G. Amar, *Phys. Rev. E* **80**, 041602 (2009).
- [27] As discussed in the text, for the special case of point islands ($d_f = \infty$) with $d \geq 2$, one has $\mu_c = 1$ and $\delta = 0$ ($\delta' = 2 - 2/\mu$) for $\mu \geq 1$ ($\mu \leq 1$).
- [28] L. H. Tang, *J. Phys. I (France)* **3**, 935 (1993).
- [29] G. S. Bales and D. C. Chrzan, *Phys. Rev. B* **50**, 6057 (1994).
- [30] Note that Eq. (18) in Ref. [26] is actually for χ' rather than for χ .
- [31] P. Lévy, *Théorie de L'addition des Variables Aléatoires* (Gauthier Villars, Paris, 1937).
- [32] J. G. Amar, F. Family, and D. C. Hughes, *Phys. Rev. E* **58**, 7130 (1998).
- [33] For the case of normal diffusion corresponding to $\mu = 1$, the hopping direction was chosen randomly after each step.
- [34] T. A. Witten and L. M. Sander, *Phys. Rev. Lett.* **47**, 1400 (1981).
- [35] P. Meakin, *Phys. Rev. B* **29**, 3722 (1984).
- [36] J. G. Amar, F. Family, and P.-M. Lam, *Phys. Rev. B* **50**, 8781 (1994).
- [37] For $\mu \geq 1.5$ the measured value of d_f for ramified islands was between 1.9 and 2.0.
- [38] M. C. Bartelt and J. W. Evans, *Phys. Rev. B* **46**, 12675 (1992).
- [39] The slightly lower effective value of χ for $\mu = 1$ shown in Fig. 3 compared to Fig. 2 is most likely due to the fact that we have used a continuous-time random walk with $\mu = 1$ rather than a simple random walk in this case.
- [40] E. Sabbar and J. G. Amar (unpublished).
- [41] N. Kumar, U. Harbola, and K. Lindenberg, *Phys. Rev. E* **82**, 021101 (2010).
- [42] N. N. Poddar and J. G. Amar (unpublished).
- [43] J. A. Blackman and P. A. Mulheran, *Phys. Rev. B* **54**, 11681 (1996).
- [44] J. G. Amar, M. N. Popescu, and F. Family, *Surface Sci.* **491**, 239 (2001).
- [45] F. Shi, Y. Shim, and J. G. Amar, *Phys. Rev. E* **74**, 021606 (2006).